

## Evaluation of the temperature-dependent dielectric function in the valence band of zinc-blende-type semiconductors

David Yevick

*Department of Electrical Engineering, Penn State University, 121 Electrical Engineering East, University Park, Pennsylvania 16802 and Institutionen för Teoretisk Fysik, Lunds Universitet, Sölvegatan 14a, S-223 62 Lund, Sweden*

Witold Bardyszewski

*Institute of Theoretical Physics, University of Warsaw, Hoza 69, PL-00-681 Warsaw, Poland*

(Received 2 December 1988)

We compute the temperature-dependent dielectric function within the context of the random-phase approximation for the  $p_{3/2}$ -symmetry valence band of semiconductors with a zinc-blende structure. Our results for the spectral density function differ considerably from previously published models and demonstrate that, with increasing temperature, the plasmon and phonon poles become markedly less damped by inter-valence-band transitions.

### INTRODUCTION

Calculations involving the hole plasma in  $p$ -type zinc-blende semiconductors have previously employed various approximations for the momentum- and energy-dependent dielectric function, each motivated by special physical considerations. The simplest of these is the plasmon-pole approximation in which the hole gas is assumed to oscillate at an undamped, temperature-independent frequency determined by a fit to the dispersion relation for plasmons at low momentum transfer  $q$ , and to that for electron-hole-pair excitations at high  $q$ .<sup>1</sup> Alternatively, at zero temperature the dielectric function may be calculated in the random-phase approximation (RPA), leading to the Lindhard expression.<sup>2</sup> Phonon effects and in particular the plasmon-phonon modes may then be modeled by adding an appropriate lattice polarization term. Neither of these methods, however, incorporate the fact that plasma oscillations in  $p$ -type zinc-blende-structure semiconductors can excite inter-valence-band transitions giving a finite lifetime to the plasmon.<sup>3</sup> In the damped-plasmon-pole model, the plasmon-pole model is accordingly modified by the inclusion of a phenomenological damping factor of the order of the plasma frequency.<sup>4</sup> Further, the  $T=0$  RPA dielectric function may still be evaluated analytically if a more exact treatment is desired.<sup>5</sup> Although the detailed structures of the damped plasmon pole and the RPA spectral density functions differ considerably, both fulfill appropriate sum rules and the effective widths of the damped-plasmon resonances roughly coincide.

While the above models are only applicable to  $T=0$ , interest has recently been focused on the finite-temperature dielectric function by room-temperature Raman-scattering measurements of the plasmon-phonon mode line shapes in highly excited InP.<sup>6</sup> These line

shapes were subsequently compared to an analytic expression for the finite-temperature dielectric function in the limit of vanishing momentum transfer  $q$ .<sup>5</sup> In this paper, we extend this analysis to arbitrary  $q$  and further explore physical implications in detail. We find that at temperatures for which the holes in the valence band are nondegenerate, the finite- and zero-temperature dielectric functions diverge markedly. In fact, since the holes are now widely distributed in energy, at a given frequency only a small number may participate in intersubband transitions. The collective excitation peaks in the spectral density function therefore sharpen rapidly with increasing temperature. These findings confirm previous, largely unreported results.<sup>7,8</sup>

### THEORETICAL METHOD

The starting point for our analysis is the following expression for the dielectric function:

$$\epsilon(q, \omega) = \epsilon_{\infty} + \Delta\epsilon^{\text{latt}}(q, \omega) + \Delta\epsilon^{\text{inter}}(q, \omega) + \Delta\epsilon^{\text{intra}}(q, \omega). \quad (1)$$

The four terms in the above expression originate from the core and lattice electrons, and from interband and intraband transitions, respectively. Introducing the longitudinal- and transverse-optical-phonon frequencies,  $\omega_{\text{LO}}$  and  $\omega_{\text{TO}}$ , we obtain for the lattice-electron contribution

$$\Delta\epsilon^{\text{latt}}(q, \omega) = \epsilon_{\infty}(\omega_{\text{LO}}^2 - \omega_{\text{TO}}^2) / (\omega_{\text{TO}}^2 - \omega^2). \quad (2)$$

In atomic units, the RPA expressions for the dielectric functions in the valence band may be written with the aid of the  $\mathbf{k} \cdot \mathbf{p}$  approximation for the intraband overlap integrals as

$$\Delta\epsilon^{\text{inter}}(q, \omega) = \frac{4\pi e^2}{q^2} \sum_{\mathbf{k}} \frac{3}{2} \frac{q^2 \sin^2 \Phi}{(\mathbf{q} + \mathbf{k})^2} 2 \left[ \frac{f_L(k)[E_L(\mathbf{k}) - E_H(\mathbf{k} + \mathbf{q})]}{(\omega + i\eta)^2 - [E_L(\mathbf{k}) - E_H(\mathbf{k} + \mathbf{q})]^2} + \frac{f_H(k)[E_H(\mathbf{k}) - E_L(\mathbf{k} + \mathbf{q})]}{(\omega + i\eta)^2 - [E_H(\mathbf{k}) - E_L(\mathbf{k} + \mathbf{q})]^2} \right] \quad (3)$$

and

$$\Delta\epsilon^{\text{intra}}(q, \omega) = \frac{4\pi e^2}{q^2} \sum_{\mathbf{k}} \left[ 2 - \frac{3}{2} \frac{q^2 \sin^2 \Phi}{(\mathbf{q} + \mathbf{k})^2} \right] 2 \left[ \frac{f_L(k)[E_L(\mathbf{k}) - E_L(\mathbf{k} + \mathbf{q})]}{(\omega + i\eta)^2 - [E_L(\mathbf{k}) - E_L(\mathbf{k} + \mathbf{q})]^2} + \frac{f_H(k)[E_H(\mathbf{k}) - E_H(\mathbf{k} + \mathbf{q})]}{(\omega + i\eta)^2 - [E_H(\mathbf{k}) - E_H(\mathbf{k} + \mathbf{q})]^2} \right]. \quad (4)$$

Here the light- and heavy-hole energies are given by the standard parabolic energy-momentum dispersion relation in the spherical approximation  $E_{H,L}(\mathbf{k}) = k^2/2m_{H,L}$ . The Fermi functions with heavy- and light-hole energy arguments are similarly denoted  $f_H(k)$  and  $f_L(k)$ . The numerical evaluation of Eqs. (3) and (4) may now be performed in either of two ways. We first write

$$\Delta\epsilon^{\text{inter}}(q, \omega) + \Delta\epsilon^{\text{intra}}(q, \omega) = \frac{4\pi e^2}{q^2} [\Delta\epsilon_{L,H}(q, \omega) + \Delta\epsilon_{L,H}^*(q, -\omega) + \Delta\epsilon_{H,L}(q, \omega) + \Delta\epsilon_{H,L}^*(q, -\omega)]. \quad (5)$$

We then determine the imaginary part of the dielectric function, which may, after delta-function elimination, be expressed as a simple one-dimensional integral. Defining  $\gamma_j = m_j/m_i$  and  $k_{\min} = |(2m_i\omega + q^2)/2q|$  and denoting the lower and upper absolute values of the roots of  $[2m_j\omega + k^2(1 - \gamma_j) + q^2] = \pm 2kq$  by  $k_1$  and  $k_2$ , respectively, we find

$$\begin{aligned} \text{Im}\Delta\epsilon_{ij}(q, \omega) = & -\frac{3e^2 m_j}{8q^3} \int_{k_1}^{k_2} dk \frac{[2\omega m_j - \gamma_j k^2 + (k - q)^2][2\omega m_j - \gamma_j k^2 + (k + q)^2]}{k(2m_j\omega - k^2\gamma_j)} f_i(k) \\ & - \frac{2m_i e^2}{q^3} \int_{k_{\min}}^{\infty} dk k \left[ 1 - \frac{3}{4} \frac{(2m_i\omega + q^2)^2 - 4k^2 q^2}{(2m_i\omega - k^2)4k^2} \right] f_i(k). \end{aligned} \quad (6)$$

The real part of the dielectric function may then be obtained directly by use of the Kramers-Krönig relations. Our second, more numerically efficient procedure, however, is to recast the real part of the dielectric function into the form

$$\begin{aligned} \text{Re}\Delta\epsilon_{ij}(q, \omega) = & -\frac{3e^2 m_i}{8\pi q^3} \int_0^{\infty} dk \frac{1}{k} \left[ [(2m_j\omega - \gamma_j k^2 + k^2 + q^2)^2 - 4k^2 q^2] \ln \left| \frac{2m_j\omega - \gamma_j k^2 + (q + k)^2}{2m_j\omega - \gamma_j k^2 + (q - k)^2} \right| \right. \\ & \left. - [(2m_i\omega + q^2)^2 - 4k^2 q^2] \ln \left| \frac{q^2 + 2kq + 2m_i\omega}{q^2 - 2kq + 2m_i\omega} \right| \right. \\ & \left. - 4kq(2m_i\omega - k^2)(\gamma_j - 1) \right] \frac{f_i(k)}{k^2 - 2m_i\omega} \\ & + \frac{e^2 m_i}{\pi q^3} \int_0^{\infty} dk k \ln \left| \frac{(q^2 + 2kq)^2 - 4m_i^2 \omega^2}{(q^2 - 2kq)^2 - 4m_i^2 \omega^2} \right| f_i(k). \end{aligned} \quad (7)$$

Although evaluation of the above expressions is quite rapid, we are currently attempting to enhance further the efficiency of our procedure for high temperatures by expanding the Fermi functions into a finite-temperature series and subsequently integrating analytically.

## RESULTS

As stated earlier, our most significant finding is the decreased damping of the collective excitations with temperature. To illustrate, in Fig. 1 we show the GaAs spectral density functions calculated both from Eqs. (5)–(7) (solid line) and from the damped-plasmon-pole model (dashed line). These are plotted as functions of energy in meV for four representative values of the wave vector  $q$  at  $p = 2 \times 10^{18} \text{ cm}^{-3}$  and room temperature. Our input parameters are  $m_L = 0.082$ ,  $m_H = 0.5$ ,  $\epsilon_{\infty} = 10.91$ ,  $\epsilon_0 = 12.72$ , and  $\hbar\omega_{\text{LO}} = 36.5 \text{ meV}$ . At this concentration, the plasmon energy,  $\hbar\omega_p \equiv \hbar[2\pi p e^2 (m_H^{-1} + m_L^{-1}) / \epsilon_{\infty}]^{1/2}$ , is 42.4 meV, which nearly coincides with the longitudinal-optical-phonon energy. As a consequence,

the two excitations interact strongly over the entire energy and momentum region shown. The plasmon-pole and RPA theories diverge as expected for  $q = 0.1q_p$ , Fig. 1(a), where we have defined  $q_p \equiv (2m_L \tilde{\omega}_p / \hbar)^{1/2} = 3.0 \times 10^6 \text{ cm}^{-1}$  with  $\tilde{\omega}_p^2 \equiv 4\pi e^2 p [(m_1^{1/2} + m_2^{1/2}) / (m_1^{3/2} + m_2^{3/2})] / \epsilon_{\infty}$ , as a result of the small hole population susceptible to inter-valence-band transitions for energies equal to the plasmon and phonon energies. For  $q = 0.5q_p$  and  $q = q_p$ , Figs. 1(b) and 1(c), however, electron-hole-pair production in the light-hole-band as well as inter-valence-band transitions become more probable, and the plasmon structure is therefore broadened in both approaches. At  $q = 2.0q_p$ , Fig. 1(d), the plasmon line is highly broadened while the phonon is instead effectively undamped in our model.

Next, we display the evolution of the dielectric function at  $q = 0.1q_p$  with temperature. At  $T = 0 \text{ K}$ , we obtain Fig. 2(a) for the dielectric function, which despite the differing material parameters resembles Fig. 2 of Ref. 4 if phonon effects are disregarded. At  $T = 200 \text{ K}$ , Fig. 2(b),

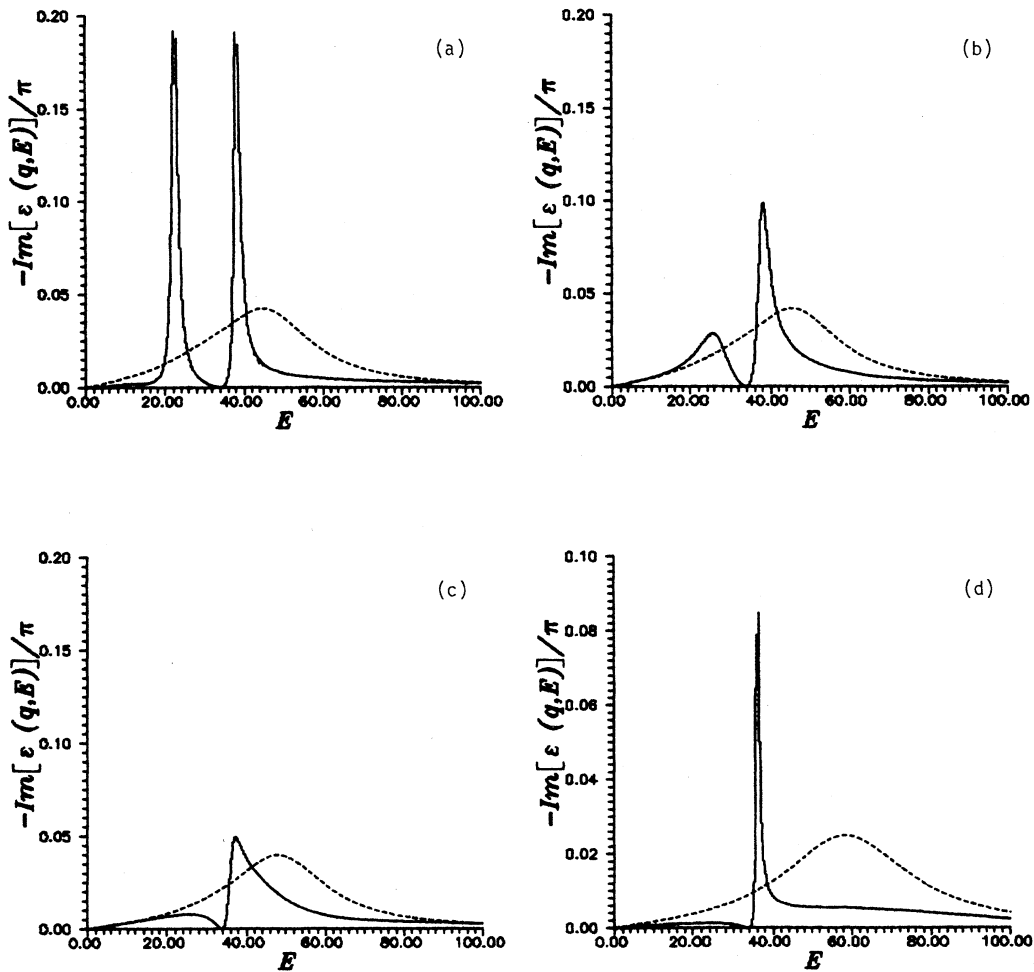


FIG. 1. The (solid line) room-temperature RPA and (dashed line) damped-plasmon-pole spectral densities, including phonon effects, as functions of energy  $E$  in meV at a hole concentration  $p = 2 \times 10^{18} \text{ cm}^{-3}$  for (a)  $q = 0.1q_p$ , (b)  $q = 0.5q_p$ , (c)  $q = q_p$ , and (d)  $q = 2.0q_p$ , where the plasmon energy  $\hbar\omega_p = q_p^2/2m_L$ .

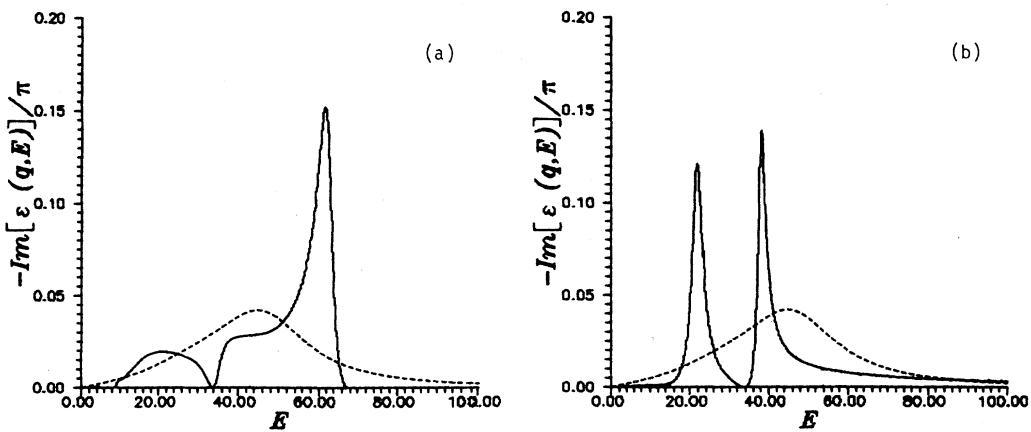


FIG. 2. The spectral densities of Fig. 1 for  $q = 0.1q_p$  but with (a)  $T = 0 \text{ K}$  and (b)  $T = 200 \text{ K}$ .

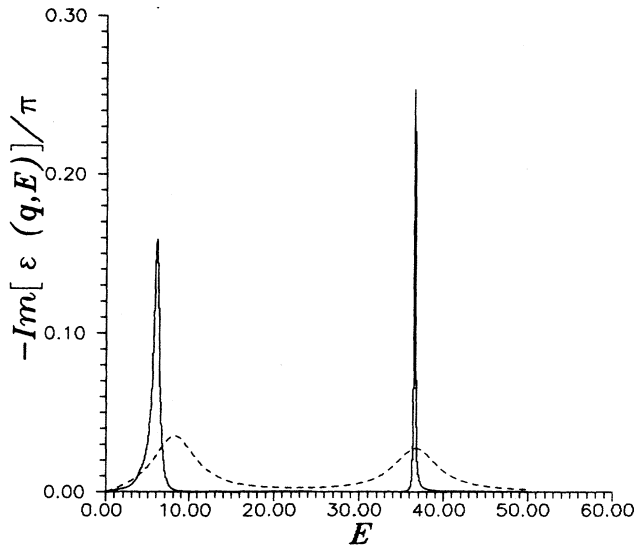


FIG. 3. As in Figs. 1 and 2, but with  $p = 1 \times 10^{17} \text{ cm}^{-3}$ ,  $q = 0.1q_p$  ( $\hbar\omega_p = 9.5 \text{ meV}$ ), and  $T = 300 \text{ K}$ .

the broadening of the spectral density has decreased noticeably, and at  $T = 300 \text{ K}$ , Fig. 1(a), an extremely sharp peak is generated. If we instead decrease the free-hole concentration to  $p = 1 \times 10^{17} \text{ cm}^{-3}$ , we produce Fig. 3. Here we observe two important effects. First, since the plasmon energy,  $\hbar\omega_p = 9.5 \text{ meV}$ , is proportional to the square root of the excess carrier concentration, the plasmon and phonon poles are far more widely separated than in Figs. 1 and 2. Secondly, as the carrier concentration is lowered, the Fermi level is increasingly displaced from the top of the valence band, so that the hole gas becomes less degenerate. The plasmon and phonon peaks are therefore further sharpened, augmenting the disagreement between the damped-plasmon-pole approximation and the RPA dielectric function. Finally, in Fig. 4 we present curves for the spectral density function in the absence of phonon effects. This curve, which again relates to  $p = 1 \times 10^{17} \text{ cm}^{-3}$ ,  $q = 0.1q_p$ , and  $T = 300 \text{ K}$ , illustrates in isolation the temperature-induced spectral line narrowing of the plasmon peak.

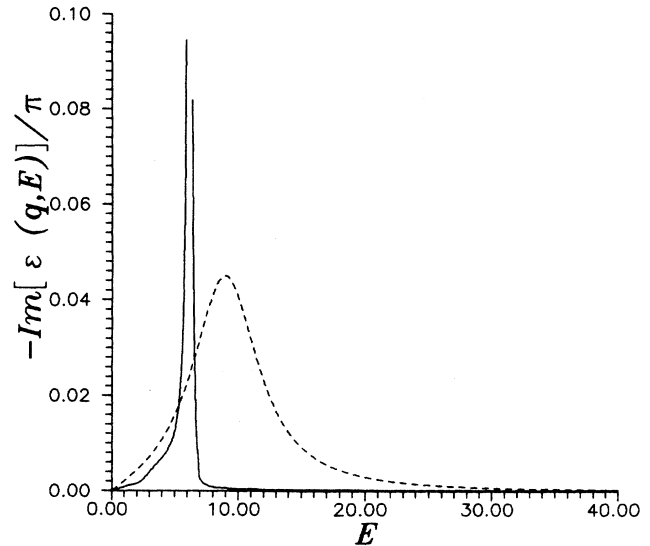


FIG. 4. As in Fig. 3 but in the absence of phonon effects.

## CONCLUSIONS

We have evaluated numerically the exact finite-temperature RPA dielectric function within the framework of a realistic model for the valence band of zincblende semiconductors. Our results confirm earlier, primarily unpublished results<sup>6,7</sup> which indicate that the dielectric function is strongly temperature dependent and consequently that zero-temperature models cannot in general be applied to the calculation of room-temperature effects. In parallel papers we have quantified this statement by determining the difference in the band-gap renormalization and the inelastic electron lifetime in *p*-type GaAs determined from the finite-temperature RPA dielectric function and from the damped-plasmon-pole model.<sup>9,10</sup>

## ACKNOWLEDGMENTS

The authors wish to thank the Swedish National Council for Applied Research (STUF) and the Polish Ministry of Science, Higher Education, and Technology (Grant No. CPBP-01-03) for financial support, and Jeff Young for valuable conversations.

<sup>1</sup>A. W. Overhauser, Phys. Rev. B **3**, 1888 (1971).

<sup>2</sup>J. Lindhardt, K. Dan. Vidensk. Selsk. Mat.-Fys. Medd. **28**, No. 8 (1954).

<sup>3</sup>M. Combescot and P. Nozières, Solid State Commun. **10**, 301 (1972).

<sup>4</sup>T. M. Rice, Nuovo Cimento B **23**, 226 (1974).

<sup>5</sup>W. Bardyszewski, Solid State Commun. **57**, 873 (1986).

<sup>6</sup>K. Wan, J. F. Young, and A. J. SpringThorpe, Can. J. Phys. **65**, 831 (1987).

<sup>7</sup>R. März, thesis, Universität Frankfurt, 1983.

<sup>8</sup>H. Nather and L. G. Quagliano, J. Luminesc. **30**, 50 (1985).

<sup>9</sup>W. Bardyszewski and D. Yevick, Phys. Rev. B **39**, 5861 (1989).

<sup>10</sup>W. Bardyszewski and D. Yevick, Appl. Phys. Lett. (to be published).